quaternary

MDPI

Article

# A Macroscopic Charcoal and Multiproxy Record from Peat Recovered from Depression Marshes in Longleaf Pine Sandhills, Florida, USA

**Benjamin Tanner [1,*], Morgan Douglas [2], Cathryn H. Greenberg [3], Jessica Chamberlin [1] and Diane Styers [2]**

[1] Department of Environmental Science and Studies, Stetson University, Deland, FL 32723, USA; jnchambe@stetson.edu
[2] Department of Geosciences and Natural Resources, Western Carolina University, Cullowhee, NC 28723, USA; morganleedouglas@gmail.com (M.D.); dmstyers@email.wcu.edu (D.S.)
[3] Southern Research Station, United States Forest Service, Department of Agriculture, Asheville, NC 28804, USA; kgreenberg@fs.fed.us
* Correspondence: btanner@stetson.edu; Tel.: +1-386-822-7382

Academic Editor: Valentí Rull
Received: 8 October 2018; Accepted: 13 November 2018; Published: 19 November 2018


**Abstract:** Science-based information on historical fire frequency is lacking for longleaf pine sandhills. We undertook a high-resolution macroscopic charcoal and geochemical analysis of sediment cores recovered from three depression marshes located within a longleaf pine sandhill ecosystem in Florida, USA. A ~1500-year fire history reconstructed from >1.5 m length peat cores analyzed at decadal to multi-decadal resolution revealed abundant macroscopic charcoal particles at nearly all sampling intervals, suggesting that fire occurred near the sites for almost all decades represented in the deposit. This result supported previous hypotheses of a frequent natural fire return interval for Florida's longleaf pine sandhills and suggested that management decisions for this ecosystem should continue to focus on the frequent prescription of controlled burns. Our research also demonstrated that some of Florida's depression marshes contain a >3000-year archive of organic-rich peat. Bulk elemental carbon and nitrogen data and stable carbon isotope analysis of the deposits at two of the three study sites suggested persistently wet soils. Soil data from the third site suggested that drying and peat oxidation occurred periodically. These depression marshes rapidly sink carbon, with measured sequestration rates on the order of 16 to 56 g $m^{-2}$ $yr^{-1}$. Our research demonstrated that Florida's depression marshes provide an untapped record of paleoenvironmental information.

**Keywords:** depression marsh; charcoal; multiproxy; fire regime; longleaf pine sandhills

## 1. Introduction

Depression marshes are scattered throughout much of the Southeastern US xeric, longleaf pine (*Pinus palustris*)-wiregrass sandhills ecosystem. This ecosystem is dependent on frequent, low-intensity fire that impedes encroachment of hardwood trees, maintaining an open forest structure that supports a diverse suite of plant and animal species [1]. The assumption of a historical, frequent fire return interval is based on ecological studies and descriptions by early explorers [1], with little science-based information on historical fire frequency or the driving climatic factors, at a local-level. Historical range of variation in longleaf pine fire regimes, and how it varied in relation to climate, has never been substantiated by paleoenvironmental analysis of the sediment archives within wetlands such as the depression marshes in Florida [2].

Forest managers need a reference condition, based on the historical range of variability in natural disturbances, to guide forest and management and restoration decisions such as prescribed

burn frequencies. The historical "natural" disturbance regime—prior to human influence—is nearly impossible to gauge, as humans have inhabited and impacted the Southeastern US for thousands of years [3]. Nonetheless, increased understanding of the historical climate, wetland conditions, and fire regimes within the longleaf pine-wiregrass ecosystem is especially important in light of the biological diversity that it supports, and the predicted future climate change [4–6]. For example, hydroregimes in these depression marshes can influence the breeding success of many amphibian species, making them vulnerable to the changing weather patterns associated with climate change [6,7].

Despite their abundance and regional importance, almost nothing is known about the suitability of depression marshes as archives of paleoenvironmental information on past climatic conditions, or on fire frequencies within the longleaf pine-wiregrass sandhills ecosystem. However, information from other wetland types is available for the region. A diatom-based environmental reconstruction from a sinkhole lake sediment core in south Florida, along with pollen data from nearby sites, suggests that modern precipitation regimes were in place by circa (ca.) 4000 cal BP (We converted all ages from external references cited in the present paper to calibrated years before present—cal BP—, with present = AD 1950, to the best of our ability, with the caveat that sometimes the original reporting conventions are unclear) [8]. However, an oxygen isotope and ostracod record from a south Florida spring suggests significant late-Holocene shifts, with saline water intrusion resulting from dry climatic conditions between ca. 2750 and 1850 cal BP, and wetter conditions with a suggested sea level high stand at ca. 900 cal BP [9]. However, composite sea level records from the Gulf of Mexico do not support a high stand at that particular time [10–12]. Further north, a pollen and charcoal study from a peat-accumulating floodplain depression wetland in the Georgia coastal plain suggests a cooling after 4500 cal BP, with increased pine establishment and fire activity, and relatively dry but variable weather conditions [13]. A paleoenvironmental diatom-based reconstruction from an infilled oxbow pond located in the South Carolina coastal plain suggests persistent open water conditions beginning ca. 5400 cal BP, but with episodic drying of pond sediments during the Late Holocene [14]. Together, these regional studies suggest that there is a climatic regime of periodic late-Holocene drying in the southeastern Coastal Plain that has persisted to the present time. A better understanding of historical climate, hydroregime, and fire frequency may facilitate better predictions of future wetland conditions in response to a changing climate.

Several studies have linked a changing climate to changes in fire activity at a broad scale. Increased fire can result from both wetter periods that can lead to increased fuel loads, and drier and warmer periods that can promote fire spread [15]. In a global synthesis, Marlon et al. [15] showed a global increase in fire activity from 3000 to 2000 cal BP, which the authors argue resulted at least partially from climatic forcing. They then suggested that this would be one of the only mechanisms that could lead to a synchronous global increase in fire activity, even though they recognized that climate proxies do not support global changes over that time period. Marlon et al. [15] also suggested that human activity may be responsible for the 3000 to 2000 cal BP spike in fire activity, where coinciding increases in human population and cultivated area (increased agriculture) during that time led to increased biomass burning in multiple regions. This global increase in fire activity from 3000 to 2000 cal BP is not as distinct in North America, and seems to occur more gradually. This gradual increase in biomass burning occurred from the mid- to late-Holocene in North America, peaking at 2000 cal BP, but not clearly coinciding with any external climatic or anthropogenic forcing. In a separate synthesis, this increase was not seen, but the record instead showed stable fire activity over the past 5000 years in eastern North America [16]. This stability was confirmed in a fire history synthesis for the Neotropics, which showed near present activity from 6000 cal BP onwards [17]. A synthesis that included all of the Americas together showed a more recent, general decline in biomass burning that continued to the present, coinciding with the onset of the Little Ice Age [18].

Data from boreal forests show that macroscopic charcoal can resist degradation and fragmentation over millennia in many settings. Thus, macroscopic analysis represents a useful tool for studying vegetation and wildfire history [19,20]. Macroscopic particles have the potential to travel airborne for

several kilometers [21], but macroscopic (>0.5 mm) charcoal generally represents local events on the order of ~$10^1$ to $10^3$ m [22] and is therefore thought to be representative of the local fire history [23], despite their uneven distribution within burn areas [24]. Macroscopic charcoal records derived from multiple, adjacent field sites are useful for separating the effects of climatic vs. local controls on fire history [25], and global syntheses are also useful for studying climatic effects on fire history [16]. A multiproxy approach is commonly used when attempting to tease out the effects of climate on fire history [26–29]. However, even when multiple sites are studied, local controls on fire regimes often obscure the climatic effects [30]. Moreover, vegetation shifts due to climatic changes may be a more important control on fire regimes than the climatic changes themselves [28].

We used peat cores from three depression marshes in north-central peninsular Florida, to construct a multi-centennial to millennial-scale macroscopic charcoal record of the surrounding longleaf pine forest ecosystem. The xeric, sandy soils typical of longleaf pine sandhill sites result in a lack of organic-rich soils that would otherwise preserve a long record of macroscopic charcoal indicative of fire history. However, depression marshes within the longleaf forest mosaic can accumulate peat [4] and the potential macroscopic charcoal layers within it. We selected macroscopic charcoal because the processing and analysis is straightforward, and macroscopic charcoal records represent local fire histories [23]. Since little is known about the long-term hydroregime within these depression marshes, and its response to changes in the climate, our secondary goal was to establish a long-term record of wet-dry cycles within the marshes based on the multiproxy analysis of elemental C (Carbon), N (Nitrogen), macroscopic charcoal, and stable carbon isotopic composition of the peat cores recovered from them.

As summarized in Tanner et al. [31], high C/N ratios (generally above 20) are associated with vascular land plant organic matter, whereas lower C/N ratios suggest increased algal contributions (algal C/N generally between 4 and 10) and wetter conditions [32], although C/N ratios cannot always be confidently tied to vegetation changes in all environments [33]. Carbon isotope ratios of organic matter can be used as a climate proxy because the proportion of plants using the C3 ($\delta^{13}C \approx -28‰$) vs. C4 ($\delta^{13}C \approx -14‰$) photosynthetic pathway in a given setting is controlled largely by the temperature, aridity, exposure to sunlight, and atmospheric $pCO_2$. The C4 plants are more abundant when conditions are warmer, drier, or when there is low $pCO_2$ [34], and drought stress in C3 plants causes a carbon isotope fractionation and results in $\delta^{13}C$ values moving towards those associated with C4 plants [35]. Therefore, variations in $\delta^{13}C$ values of organic matter during the Holocene in locations where C4 plants are present are likely related to warmer and/or drier conditions or drought stress in C3 plants. The C4 photosynthetic pathway is commonly utilized in *Cyperaceae* and *Gramineae* species in Florida, making up 41% and 80% of those species distributions, respectively [36,37]. Therefore, significant drying of our field sites should result in the presence of increased C4 species, and a resulting increase in the $\delta^{13}C$ values. These proxies have been successfully used to infer dry periods recorded in other southeastern USA wetlands [31].

## 2. Materials and Methods

Our study wetlands were a representative selection of small (<0.4 ha), ephemeral, groundwater-driven sinkhole wetlands, embedded within the xeric longleaf pine-wiregrass sandhill uplands of the Floridan Aquifer System region, Ocala National Forest, Marion and Putnam Counties, Florida, USA (Figure 1) [7]. The longleaf pine-wiregrass sandhill ecosystem occurs on the Southeastern US Coastal Plain and is characterized by undulating topography and thick sands, leading to a xeric environment [4]. Dominant plant species are fire-adapted and include longleaf pine (*Pinus palustris*), turkey oak (*Quercus laevis*), and wiregrass (*Aristida stricta* var. *beyrichiana*). Florida's depression marshes occur statewide north of the Keys and are often present within the longleaf sandhills [4]. Depression marshes are small, seasonally-inundated, surficially-isolated wetlands with a sandy substrate, commonly with peat accumulation. These wetlands are sometimes zoned into bands related to the inundation time, into a complex mosaic of species.

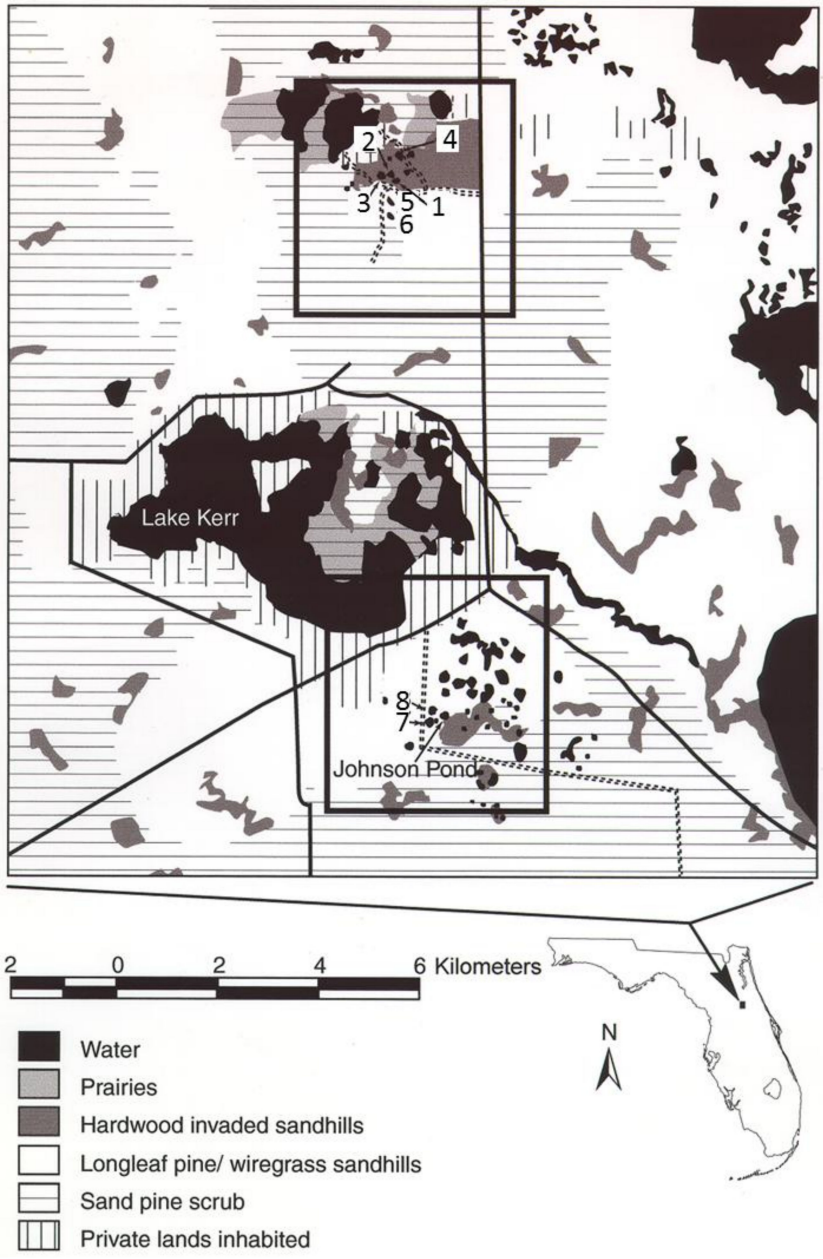


**Figure 1.** Map showing land cover types and the location of the field sites (1–8) in the Ocala National Forest in Putnam and Marion Counties, FL, USA, courtesy of Dale Johnson.

Species common to our sites include *Andropogon* spp., *Panicum hemitomum*, *Rhexia* spp., *Lachnanthes caroliniana*, and *Nymphaea odorata*, with *Cephalanthus occidentalis* encroaching on some of the sites. Annual precipitation (1981–2010) at Ocala, Florida was 129 cm and the average daily maximum and minimum temperatures were 32.1 and 19 °C from April to October, and 24 and 9.4 °C from November to March [38].

Depression marshes within the study area are sinkholes developed within the Late Pliocene Cypresshead Formation, presumably due to the dissolution of the underlying Hawthorn Group or Ocala Limestone carbonates. The Cypresshead Formation, which is present at the surface at our field sites, is typified by fine to very coarse quartz sands with common occurrences of quartz gravel and minor kaolinite clay [39]. Some of the studied depression marshes accumulate peat and this wetland peat overlies Astatula Sand, which, along with Tavares Sand, blankets the region surrounding the field sites. Astatula and Tavares Sands are classified as Hyperthermic, uncoated Typic Quartzipsamments,

which form on knolls, dunes, or ridges on the marine terraces in xeric uplands [40]. These soils are excessively drained, with saturated hydraulic conductivity ($K_{sat}$) values falling between 15 and 127 cm $hr^{-1}$. The depth to a restrictive feature is >2 m. Only A and C horizons are typically present and both are usually composed primarily of sand [40].

We selected three (sites 1, 5, and 8) of eight depression marshes used in a long-term (>24 yr) study of amphibian ecology and hydroregime [6], based on depth of the organic peat accumulation and the distance apart (Figures 1 and 2). As part of the long-term study, water levels and precipitation have been continuously monitored at each site beginning in 1994 [7]. Local precipitation was measured using a rain gauge placed out in the open near site 1, daily from 28 March 1994 through to mid-2006, and approximately three times weekly thereafter. Water depth was measured approximately weekly at each wetland using PVC staff gauges that were permanently established at the approximate lowest point within the individual wetland basins. Soil cores were removed from each site in January 2016 using a half spoon, 1 m length gouge auger (Eijkelkamp North America Inc., Morrisville, NC, USA) that did not compact the sediments. Successive 3 cm or 6 cm diameter core sections were recovered from each site and the coring proceeded to refusal (sand). Cores were described in the field for visible characteristics, including color, texture, and the degree of decomposition. Sediment cores were kept waterlogged, placed in 1 m length plastic tubes, wrapped in plastic, and transferred to the core lab at Western Carolina University for immediate processing.

**Figure 2.** Photograph of site 5 during core work showing the depression marsh and the surrounding longleaf pine/wiregrass sandhill community, courtesy of Gabriel Kamener.

The core sections were cleaned (i.e., edge sediments scraped off) in the lab to expose fresh sediments for subsampling. Sampling proceeded from the interior of the core to avoid contamination. Cores were sub sampled using a 1.5 cm diameter plastic syringe with volume indicators for bulk density, carbon and nitrogen content, and for stable carbon isotope measurements. Subsample volume was recorded and samples were dried in a gravity convection oven at 65 °C to a constant weight. Dry weight was recorded, and the samples were powdered and then stored frozen until analysis. The soil cores were separately sampled for macroscopic charcoal at 1 cm intervals using a 1.5 cm diameter plastic syringe by sampling along the long axis of the cores, beginning at the core base. The syringe was inserted 1 cm into the core and the volume of sediment was recorded. The remaining portion of that sample interval was then sliced off of the core using a blade. The next 1 cm interval was then sampled as described above and the process was repeated for the full length of the core. Samples were transferred to vials and were then further processed for macroscopic charcoal. Only the first recovered section

of each core (top~1 m) was analyzed for macroscopic charcoal due to the significant time required to count charcoal at 1 cm intervals for 3 cores (with many counts >1000 pieces/sample). Organic-rich peat was removed from each core for radiocarbon analysis. Site 1 was revisited in May 2017, because insufficient material was recovered during the initial coring. Successive cores were removed directly adjacent to the original coring location and these cores were processed and subsampled at Stetson University's Environmental Science Laboratory using the already established methods.

Multiple samples from all three sites were sent to International Chemical Analysis for radiocarbon dating of the bulk peat. Indicated sample depths (see Table 1) represent the mid-point of the peat sections sent for analysis. Radiocarbon analysis was performed by following standard procedures for organic sediments, and the calibrations were calculated using CALIB Rev. 7.1.0 (Stuiver, Reimer, and Reimer, Belfast, United Kingdom) and the IntCal13 calibration database [41]. These standard procedures included examination of the samples and manual removal of contaminants like rootlets during the physical pretreatment. Additionally, samples underwent Acid–Alkali–Acid pretreatment, which included acid (HCl) treatment to remove acid soluble compounds and secondary carbonates, as well as a base (NaOH) treatment to remove humic acids, and a final acid treatment (HCl) to eliminate atmospheric $CO_2$. Linear interpolation was used to assign ages between the dated horizons, and the age /depth models were based on the mid-point of the sediment section used for radiocarbon analysis and the median, 2σ age in cal BP (present = 1950). Most of the radiocarbon ages were determined for the cores recovered during the 2016 field season (ICA 16 laboratory numbers in Table 1). Two additional radiocarbon dates were obtained for the core recovered from site 1 in 2017 (ICA 17 laboratory numbers in Table 1). This core was recovered directly adjacent (within 1 m) to the core recovered from site 1, which was also dated.

**Table 1.** Radiocarbon data are presented for the three sites. Sample depths are in cm below the ground surface and the calibration procedures are described in the Methods section.

| Sample Depth (cm) | Conventional Radiocarbon Age ($^{14}$C yr BP) | Calibrated 2σ Range (cal BP) | Calibrated 2σ Range Median (cal BP) | Dated Material | Laboratory # |
|---|---|---|---|---|---|
| **Site 1** | | | | | |
| 50 | 290±20 | 297 to 330<br>358 to 430 | 393 | peat | ICA 16P/0520 |
| 92.5 | 1810±30 | 1628 to 1667<br>1692 to 1822 | 1750 | peat | ICA 17O/0514 |
| 132.5 | 3420±30 | 3583 to 3725<br>3751 to 3761<br>3793 to 3820 | 3668 | peat | ICA 17O/0513 |
| **Site 5** | | | | | |
| 52.5 | 450±30 | 472 to 535 | 509 | peat | ICA 16P/0272 |
| 92.5 | 1430±30 | 1293 to 1375 | 1328 | peat | ICA 16P/0273 |
| 139.5 | 2310±30 | 2185 to 2195<br>2202 to 2233<br>2306 to 2359 | 2337 | peat | ICA 16P/0274 |
| 229.5 | 1520±30 | 1341 to 1424<br>1428 to 1444<br>1454 to 1522 | 1404 | peat | ICA 16P/0275 |
| **Site 8** | | | | | |
| 47.5 | 3700±30 | 3930 to 3944<br>3967 to 4100<br>4114 to 4147 | 4038 | peat | ICA 16P/0521 |

Samples were processed for macroscopic charcoal counting using standard methods described in Reference [42]. Briefly, the samples were soaked in a 3% solution of cosmetic grade $H_2O_2$ for 24 h in order to bleach the non-charcoal organic sediments to aid in the identification of charcoal particles, as in Reference [43]. Samples were then passed through nested 240 µm and 120 µm sieves using water. The 120 µm fraction was transferred to a petri dish, air dried, and then counted using a binocular

microscope at a 10–40× magnification. Charcoal counts were used to estimate the fire history instead of the area or volume tabulations, as the method was simpler and research has shown that the three proxies provide comparable results [44]. Macroscopic charcoal from only one size class was quantified because multiple studies have shown that only limited additional information is gained from studying multiple size classes, noting that the time required for the additional analysis is significant [42,45]. Total charcoal counts were converted to CHAR by dividing the counts by sample volume and multiplying by the sedimentation rate determined for the sample interval.

Powdered samples were measured for total organic carbon, nitrogen, and carbon isotope composition ($\delta^{13}C$) using a Costech Elemental Analyzer (Costech Analytical Technologies Inc., Valencia, CA, USA) coupled to a Thermo-Finnigan Delta+ XL Mass Spectrometer (Thermo Finnigan LLC, San Jose, CA, USA) at the University of Tennessee's Department of Earth and Planetary Sciences Stable Isotope Laboratory (cores from sites 5 and 8) or a Costech Elemental Analyzer coupled to a Thermo Delta V Plus Mass Spectrometer (Thermo Scientific, Waltham, MA, USA) at the University of North Carolina Wilmington's Center for Marine Science Isotope Ratio Mass Spectrometry Core Facility (cores from site 1). The depression marsh field sites are mildly acidic freshwater systems, where no carbonate has been observed. Therefore, the measured bulk carbon percentages and isotope values were assumed to represent organic contributions to the wetland sediments, and acid pretreatment was not undertaken in order to avoid possible effects on the measured isotope ratios, as outlined in Reference [46]. All $\delta^{13}C$ values were reported relative to the V-PDB standard.

Charcoal records from sites 1 and 5 were separated into background and peak components and a threshold was used to identify "fire events" of one or more fires within ~1 km (related to the typical maximum travel distance of macroscopic charcoal) of the sample site using statistical analysis with CharAnalysis software (freely available at http://CharAnalysis.googlepages.com) [28,44,47]. Briefly, the charcoal data were interpolated to time steps that corresponded approximately to the median temporal resolution of each record for sites 1 and 5 separately. A low frequency background component was subtracted from the interpolated charcoal distribution to construct a residual series (charcoal peaks). A Gaussian mixture model was used to identify noise, which can result from sediment mixing, sampling, analysis, and through other natural processes. The 99th percentile of the noise distribution was used as a threshold to separate the distribution into fire and non-fire events. Background was estimated using a locally weighted regression and a 600-year window, which was chosen to maximize the signal/noise index and the goodness of fit between the empirical and modeled noise distributions. The statistical analysis was not attempted for site 8 because of poor age control.

## 3. Results

Precipitation and water (stage) level data for sites 1, 5, and 8 are shown in Figure 3. Temporal stage levels for sites 1 and 5 were similar and our measurements showed that the wetlands were usually submerged, with five brief dry-downs over the 22-year monitoring history. Sites 1 and 5 were dry during the May 2017 core sampling site visit, but the soils were saturated to the surface despite the dry conditions. Rainfall pulses precede the water stage level increases at the sites by weeks to months (Figure 3). Precipitation totals are dominated by early June through late September rainfall and water tables at the sites, and generally reach the highest point in October and are lowest in late May and early June (Figure 3). This stage level data were published in part by Greenberg et al. [7].

Successive core sections were recovered from site 1 to a depth of 167 cm. Organic-rich peat was present near the surface and decomposition increased with depth (Table 2). Mineral-rich sediment with a high sand content was described near the base of the core (147 to 167 cm). This sandy section was not analyzed for C, N, or $\delta^{13}C$ because it was below the wetland deposition. Successive core sections were recovered from site 5 to a depth of 245 cm. Organic-rich peat was present near the surface and decomposition generally increased with depth (Table 2). Mineral-rich sediment with a high sand content was described near the base of the core. A single core section was recovered from site 8 to a depth of 57 cm. The sediments below 57 cm could not be retained even though the auger

penetrated to a greater depth. Organic-rich peat with moderate decomposition was present near the surface and highly decomposed peat was present at the base of the recovered core section (Table 2).

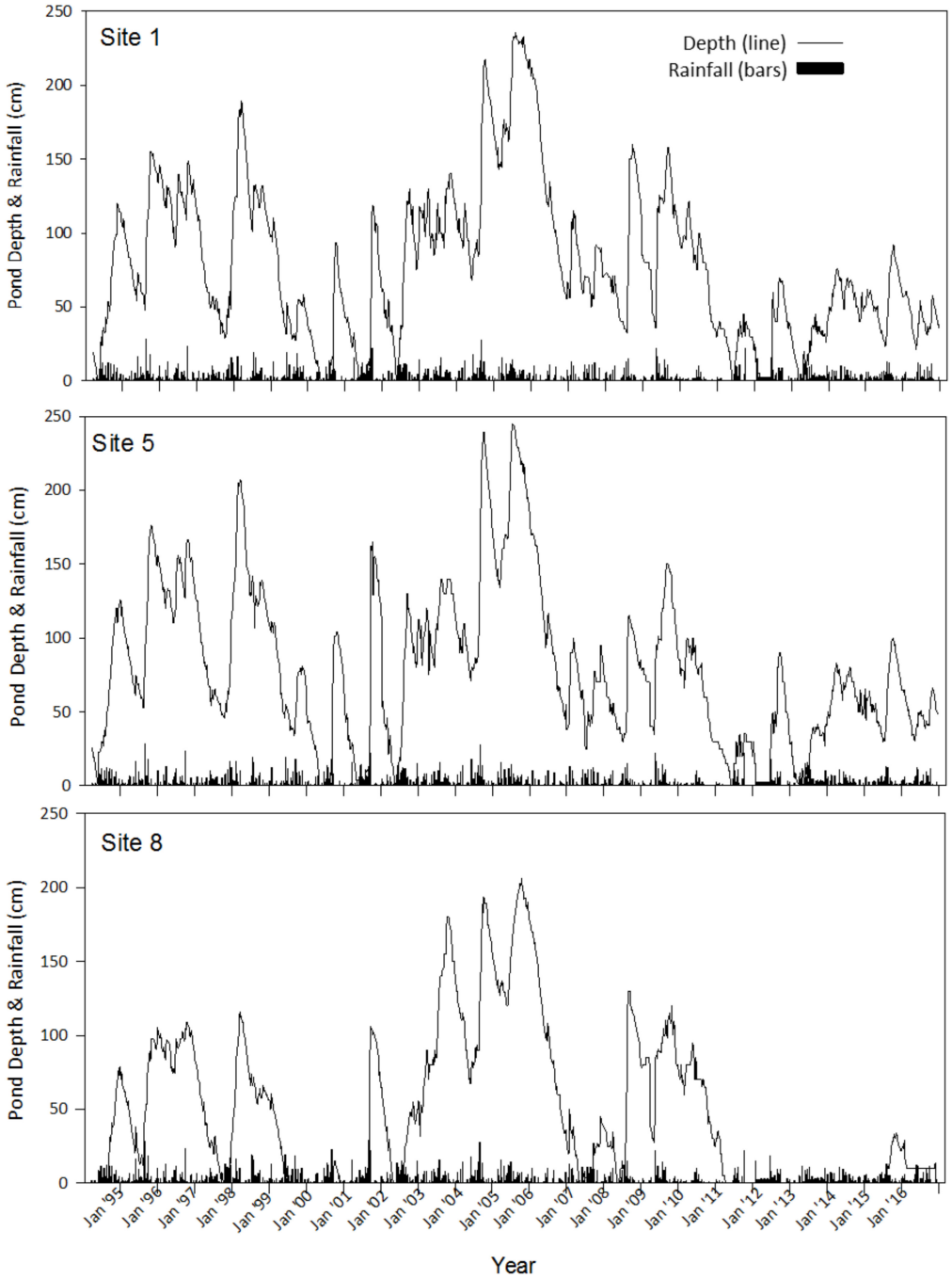


**Figure 3.** Rain gauge totals and stage level data for sites 1, 5, and 8 covering 1994 through to 2016.

**Table 2.** General soil description with soil color determinations and visible degree of peat decomposition with depth. Visible and textural mineral soil presence is mentioned when present.

| Depth Range (cmbs) | Munsell Soil Color | General Description |
|---|---|---|
| **Site 1** | | |
| 0 to 35 | 7.5YR 2.5/3 | Peat/Minimal Decomposition |
| 35 to 97 | 7.5YR 3/1 | Mucky Peat/Moderate Decomposition |
| 97 to 108 | 7.5YR 2.5/1 | Mucky Peat/Moderate Decomposition |
| 108 to 147 | 7.5YR 2.5/1 | Muck/High Decomposition |
| 147 to 167 | 7.5YR 2.5/1 | Mucky Mineral/Higher Sand Content |
| **Site 5** | | |
| 0 to 35 | 10YR 3/2 | Peat/Minimal Decomposition |
| 35 to 75 | 10YR 2/1 | Muck/High Decomposition |
| 75 to 94 | 7.5YR 3/2 | Mucky Peat/Moderate Decomposition |
| 94 to 220 | 10YR 2/1 | Muck/High Decomposition |
| 220 to 245 | 7.5YR 3/1 | Mucky Mineral/Higher Sand Content |
| **Site 8** | | |
| 0 to 8 | 7.5YR 2.5/2 | Peat/Minimal to Moderate Decomposition |
| 8 to 22 | 7.5YR 2.5/2 | Mucky Peat/Moderate Decomposition |
| 22 to 57 | 10YR 2/1 | Muck/High Decomposition |

Radiocarbon data for the three sites are presented in Table 1 and the age/depth curves are shown for sites 1 and 5 in Figure 4. An age depth curve is not presented for site 8 because only one age determination was obtained from near the base of the 57 cm length of sediment recovered, i.e., at 47.5 cm. The 2σ median age for site 1 was 3668 cal BP at 132.5 cm, being the deepest core depth sampled (out of a total core depth of 167cm) for radiocarbon age determination (Figure 4a). Tentative sedimentation rates determined though linear interpolation (Table 3) were highest near the surface (0.11 cm $yr^{-1}$) and declined with depth (0.02 cm $yr^{-1}$ for deepest core section). The basal age measured for site 5 was out of stratigraphic order (Table 1, Figure 4b). This age determination was rejected and was not used in the linear interpolation presented in Figure 4b or in the sedimentation rate measurements reported in Table 3. The deepest core section (Section 3) from site 5 (180 to 245 cm depth) was not analyzed for charcoal, C, N, or $\delta^{13}C$ because of the possible contamination revealed by the sole radiocarbon date recovered from that core section. The 2σ median age for site 5 was 2337 cal BP from the maximum 139.5 cm core depth measured for radiocarbon from the second core section (Figure 4b). Sedimentation rates determined though linear interpolation (Table 3) were highest near the surface (0.09 cm $yr^{-1}$) and declined to a steady 0.05 cm $yr^{-1}$ with depth. A single age determination was measured for site 8 at a 47.5 cm depth (total core depth = 57 cm), yielding a 2σ median age of 4038 cal BP (Table 1).

Macroscopic charcoal was analyzed for sites 1, 5, and 8 to the base of the first core section recovered from each site (Figure 5). At site 1, insufficient material was recovered from the 0–1 cm depth for analysis. Macroscopic charcoal was counted at 1cm intervals for the remainder of the 89 cm length core section and these data are presented in Figure 5a. Charcoal was present at all site 1 sample depths, except for the 5 and 12 cm intervals. Charcoal concentrations at site 1 were generally high from ca. 100 to 600 cal BP and again from ca. 1000 to the end of the sampling at 1638 cal BP (Figure 5a). Charcoal concentrations were lowest at ca. 0 and 675 cal BP. At site 5, insufficient material was recovered from the 0–6.5 cm depth and at the 30.5, 43.5, 44.5, 48.5, and 63.5 cm sample depths for analysis. Macroscopic charcoal was counted at 1cm intervals for the remainder of the 82.5 cm core section. Charcoal was present at all site 5 sample depths, except for the 21.5 to 24.5 cm intervals. Charcoal concentrations were generally high from ca. 300 to 500 cal BP and again from ca. 675 to 900 cal BP (Figure 5b). Site 5 charcoal concentrations were lowest from ca. 160 to 275 cal BP and near the base of the core section at ca. 1100 cal BP. Insufficient material was recovered from the 0–1.5 cm depth and at the 11.5, 15.5, 25.5, 34.5, and 41.5 cm sample depths from site 8 for analysis. Macroscopic charcoal was counted at 1 cm

intervals for the remainder of the 51.5 cm length core section. Charcoal was present at all site 8 sample depths. Charcoal concentrations were generally elevated throughout the core section and were lowest at ca. 3370 cal BP (Figure 5c). Results of the statistical treatment of the charcoal data are presented in Figure 6. Eight fire events were identified in the site 1 record and seven fire events were identified in the site 5 record.

**Table 3.** Sedimentation rates are presented with soil core depth intervals for the different sites. Sedimentation rates are based on soil depth and their associated 2σ median ages in cal BP. Bulk densities and carbon percentages were averaged for those core sections and are presented along with the determined carbon sequestration rate. Carbon sequestration rates were determined by multiplying the average (Avg.) sedimentation rate by the average bulk density and the average carbon percentage (as a decimal).

| Depth Range (cmbs) | Avg. Sedimentation Rate (cm $yr^{-1}$) | Avg. Bulk Density (g $cm^{-3}$) | Avg. Carbon % | Carbon Sequestration Rate (g C $m^{-2}$ $yr^{-1}$) |
|---|---|---|---|---|
| **Site 1** | | | | |
| 0 to 50 | 0.11 | 0.1 | 51 | 56 |
| 50 to 92.5 | 0.03 | 0.11 | 54 | 18 |
| 92.5 to 145 | 0.02 | 0.15 | 51 | 16 |
| **Site 5** | | | | |
| 0 to 52.5 | 0.09 | 0.08 | 50 | 37 |
| 52.5 to 92.5 | 0.05 | 0.1 | 51 | 24 |
| 92.5 to 180 | 0.05 | 0.14 | 50 | 34 |

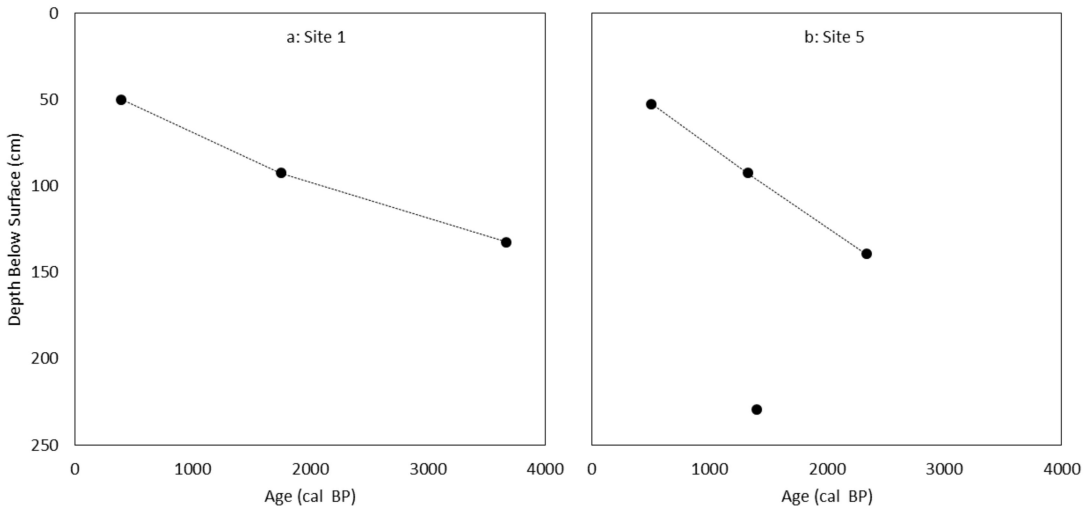


**Figure 4.** Radiocarbon age/depth curve for site 1 (**a**) and site 5 (**b**). The points represent the mid-point of the sample interval sent for radiocarbon age determination and the calibrated, 2σ median age in cal BP (present = 1950). The lines on the graphs represent the linear interpolation between dated horizons. One age determination was out of stratigraphic order for site 5 (**b**) and this age determination was not used in the age/depth model.

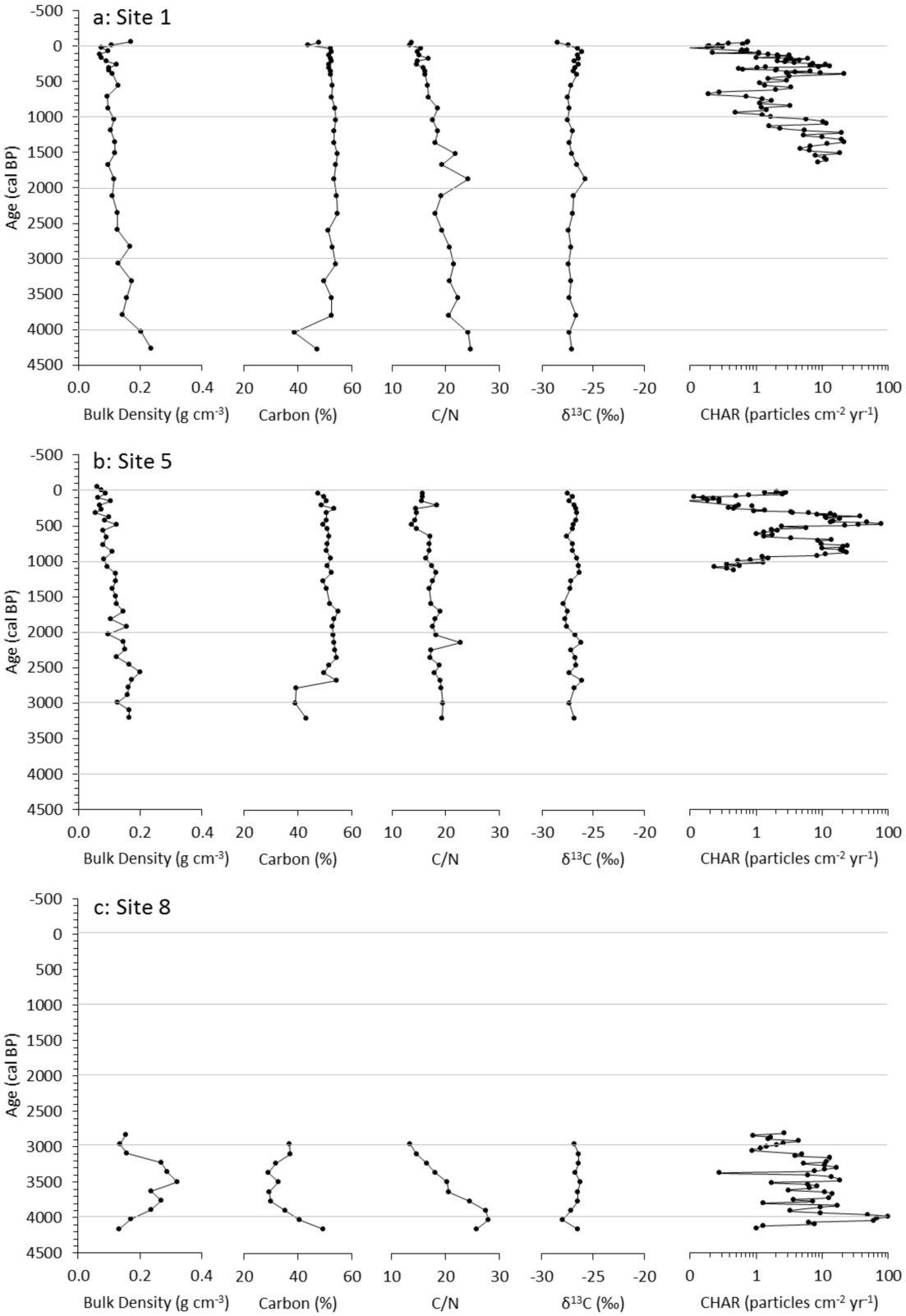


**Figure 5.** Multiproxy and CHAR data for sites 1 (**a**), 5 (**b**), and 8 (**c**) are plotted vs. age determined from the radiocarbon age control and linear interpolation between the dated horizons and the surface. Negative ages are possible because the present is defined as 1950 AD by convention. CHAR is plotted using a logarithmic scale on the *x*-axis. Only the first core section from each site was analyzed for CHAR (at 1 cm intervals).

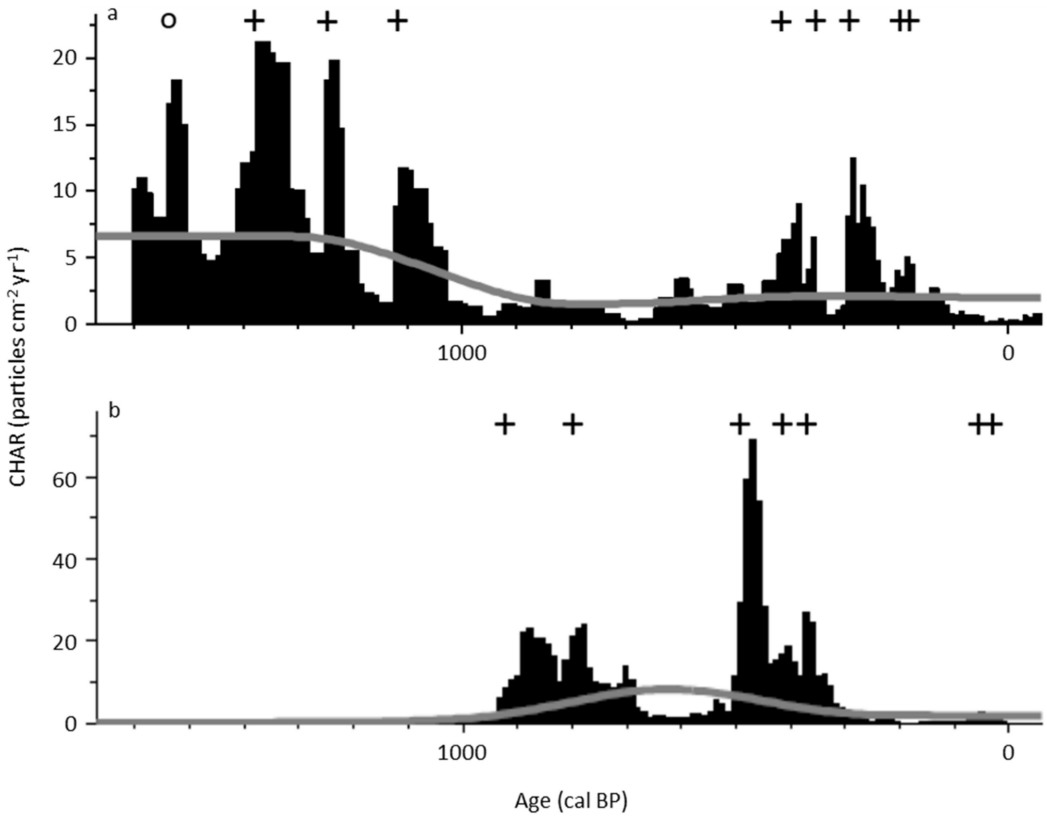


**Figure 6.** CharAnalysis statistical results for sites 1 (**a**) and 5 (**b**) showing interpolated (black) and background (grey) components along with reconstructed "fire events" ("+" symbol), identified by also taking into account noise in the charcoal distribution. Circles indicate that a peak was identified that failed the 99th percentile criterion. See Higuera et al. [28].

Bulk density measurements were generally low (below 0.2 g cm$^{-3}$) for all three sites, and these measurements increased with depth for the cores collected from sites 1 and 5 (Figure 5a,b). Bulk density values were higher for the middle of the core section recovered from site 8, increasing to above 0.3 g cm$^{-3}$ (Figure 5c). Carbon percentages were high for all the three sites and were generally above 40%. Carbon trended lower, dropping below 30%, in the middle portion of the core section recovered from site 8. C/N was near 20 down core at all 3 sites, showing a slight increase with depth. C/N ratios trended higher with depth at site 8, approaching a value of 30 near the bottom of the core. Carbon isotope ratios were low for all three sites, with the $\delta^{13}$C never increasing above −25‰ for any core depth. Sedimentation rates ranged between 0.11 and 0.02 cm yr$^{-1}$ for sites 1 and 5, showing a decline with depth at each site (Table 3). Carbon sequestration rates for the two sites varied with core depth between 16 to 56 g cm$^{-2}$ yr$^{-1}$ (Table 3).

## 4. Discussion

### *4.1. Chronology*

Many Florida lakes began to preserve sediment beginning ca. 8850 cal BP, as rising water tables flooded lake basins [2]. Our data suggested that sites 1 and 5 have been steadily accumulating peat from ca. 2500 cal BP (site 5) and ca. 3500 cal BP (site 1) to the present period (Figure 4). These age estimates could either be related to the commencement of peat accumulation at some point after the initial sinkhole formation or it could relate to the arrival of persistently wet conditions at the sites after a time of drier conditions and peat oxidation. The age/depth curves for these two sites showed a steady slope, suggesting the consistent deposition and the lack of oxidation of organic matter, which would result in the lowering of the wetland surface. This interpretation was supported by the consistently

high organic carbon percentages throughout the cores for both sites (generally above 40%) and the low bulk density values (generally below 0.2 g $cm^{-2}$, see Figure 5a,b). Significant lowering of the water table below the soil surface at the sites would likely result in the oxidation of the organic-rich peat. However, the mineral sediment fraction would remain and would concentrate as the oxidation of the peat proceeded. This process would result in higher bulk density values and lower organic carbon percentages for portions of the core, but this is not what was seen in our samples. A fire during a summer water table drawdown could potentially burn into the peat [48], and sedimentary fire history reconstructions may be complicated by peat oxidation and burning [49]. However, our data suggested that deposition was consistent and that sites 1 and 5 did not lose significant organic material due to peat oxidation and burning. No physical evidence of peat oxidation, such as abrupt changes in the degree of humification, or peat burning, such as charred soil layers, was observed in our cores. The basal radiocarbon date for site 5 (ICA 16P/0275) was out of stratigraphic order (Figure 4b, Table 1). That bottom core section was therefore not further analyzed because of the unknown age/depth relationship of those sediments.

One radiocarbon age determination was acquired for site 8 near the base of the recovered sediment section (Table 1). The median age of 4038 cal BP at the 47.5 cm sample depth suggested that either the sedimentation rate for site 8 was much lower than sites 1 and 5, or that there had been significant oxidation of the upper part of the peat profile. The latter possibility seems most likely, given the higher decomposition of organic matter nearer to the surface (Table 2) and the higher bulk density and lower percentage of carbon with depth (Figure 5c) compared to the other two sites. This also makes sense given the generally drier conditions, related to the water table being below the ground surface, recorded at site 8 over the monitoring period (Figure 3). Age control for the site 8 core is therefore suspect, and temporal comparisons of site 8 data with the other sites are dubious. Site 8 core data were plotted vs. age (Figure 5c) using the radiocarbon age of the 47.5 cm sample depth from site 8, and then by estimating the age of the other sample depths using the 50 cm to core bottom average sedimentation rate of sites 1 and 5 (=26.7 yr $cm^{-1}$). For example, the median age of the 47.5 cm sample depth was used (=4038 cal BP) and the 46.5 cm sample depth age was estimated as 4011.3 cal BP (=4038 cal BP − 26.7 yrs).

### *4.2. Water Level Monitoring*

Water level monitoring data for sites 1, 5, and 8 showed that the wetlands had a delayed response to rainfall events, suggesting that their recharge was primarily controlled by groundwater instead of direct rainfall (Figure 3). The water level data demonstrated that, over the 23-year monitoring history presented, sites 1 and 5 were primarily inundated, each drying at the surface only during 5 brief periods. This drying was nearly concurrent for the two sites. Site 8 showed prolonged dry periods, with one dry period lasting for over 4 years. These prolonged dry intervals explain why the site 8 age/depth relationship is distinctly different from the other two sites (Figure 5). Site 8 likely experienced significant peat oxidation as a result of the prolonged dry conditions. Sites 1 and 5 were dry at the surface during the site visit in May 2017, which was during a drought. Soil cores taken during that visit showed that the soils at those sites were saturated to the surface despite the lack of inundation. Soil saturation despite inundation may explain why sites 1 and 5 had steady peat accumulation, even with periodic drying at the surface. Carbon/nitrogen ratios and the $\delta^{13}C$ values of the core sediments supported the interpretation of persistent soil saturation at sites 1 and 5. C/N ratios and $\delta^{13}C$ measurements of sediments can be used to infer contributions of algal vs. aquatic vascular plants and terrestrial vegetation to wetland environments through time [50].

### *4.3. Carbon and Nitrogen*

The C/N record of the cores from both sites 1 and 5 suggested a mixture of both algal and higher plant contributions for almost all the sample depths, with C/N ratios generally falling between 14 and 20 (Figure 5a,b). The presence of some algal contribution for these sample depth intervals suggested

wet conditions. This interpretation of a wet environment through time is supported by the $\delta^{13}C$ values of the core sediments, which were all lower than −25‰, suggesting primary contributions from C3 plants that were not water stressed (Figure 5a,b). The C/N ratios increased steadily with depth for both sites. Degradation and decomposition of organic matter can result in higher C/N ratios as proteinaceous components are diminished [51], and this may explain the steady increase with depth, since it is expected that there is increasing decomposition with increased sediment age. The $\delta^{13}C$ values remained relatively constant with depth. This suggested that the C/N ratio increase with depth was due to decomposition rather than the drying of the sites and a resulting increase in higher plant abundance, which would also likely result in increasing C4 plant contributions to the sediments. There was a coincident trend of increased C/N and slightly increased $\delta^{13}C$ values at site 1 around 1850 cal BP (Figure 5a). A similar trend could be seen in the site 5 record around 2150 cal BP (Figure 5b). This shift to higher C/N and $\delta^{13}C$ values could indicate drier conditions at that time. However, there was no coincident increase in bulk density, which indicates that, if present, the possible drier conditions at that time did not lead to significant peat oxidation. Site 8 also showed consistently low $\delta^{13}C$ values and an increasing trend of C/N with depth (Figure 5c). It was difficult to interpret the site 8 record given the poor age control for the site.

The increased C/N and $\delta^{13}C$ values at sites 1 and 5 near 2000 cal BP are supported by an ostracod record from south Florida, which showed saline water intrusion in a spring resulting from dry climatic conditions between ca. 2750 and 1850 cal BP [9]. Pollen records from the Everglades suggest century-scale droughts at ca. 1000 and 400 cal BP [52], but this trend is absent in the paleoenvironmental record from sites 1 and 5. Our record also failed to resolve a severe drought around the 560s CE (approximately 1390s cal BP) present in a tree ring record associated with the Suwannee River, FL [53], although this was not surprising given that our sediment record lacked the resolution of a dendrochronological record. Oxygen isotopic and micropaleontological records from ocean sediment cores from the northern Gulf of Mexico show a warm, relatively stable Late Holocene [54], with some century scale variability related to solar forcing after a warmer, wet Mid Holocene [55]. General Late Holocene stability in the vicinity of our sites was supported by our data.

A pollen record from Lake Tulane, FL shows much variability in the forest composition over the past 50,000 years. A stable forest is represented in the Late Holocene and the authors conclude that the modern pine forest developed ca. 5750 cal BP under a regime of increased winter temperatures [2,56]. The pollen record from Mud Lake, FL, located approximately 10 miles south of our field site, also shows the establishment of the pine forest with hammocks of mesic broad-leaved trees after ca 5800 cal BP, with a possible warmer and drier climate before that time [57,58]. The pollen records from Sheelar Lake, located approximately 30 miles north of our field site, and Camel Lake (Florida panhandle) also showed the establishment of the pine forest over the latter half of the Holocene, coinciding with the modern climate of dominant summer precipitation from thunderstorms [2,59]. The modern long-leaf pine/turkey oak forest appears to have been in place by ca. 8550 cal BP in northwest Florida [60].

### *4.4. Fire History*

Prior to European settlement, fires are thought to have occurred at 1–3-year intervals throughout much of Florida (including the xeric landscape surrounding our study area), and also on wetland sites such as ours, with deep histosol soils dominated by low shrubs, grasses, and sedges [48]. European settlement in east Florida occurred around 1565 AD [48], although it is unclear when and how the settlement influence affected fire regimes within our study area. The pre-European contact indigenous population would have also manipulated the fire regime [61]. The fire frequency regime for the longleaf pine savannah is also thought to be on the order of 1–3 years [62]. A tree-ring fire scar study representing >250 years in a Louisiana longleaf pine forest suggested a 2.2-year fire return interval, and the fire frequency was unrelated to drought events [63]. A separate >250-year tree-ring fire scar study in a Mississippi longleaf pine forest suggested a 2.9-year fire return interval, with fire frequencies associated with both climate and human land use activities, such as peak grazing periods and logging

activities [64]. Some studies have successfully combined the analysis of sedimentary charcoal and tree ring fire scars to assess fire histories [22,49,65]. However, attempts to determine fire history within our study area using the longleaf pine tree ring and fire scar records proved unsuccessful, as we were unable to correlate the tree ring widths necessary to establish a dendrochronological record (D. Styers, unpublished data).

The US Forest Service currently conducts prescribed burns at 3–5-year intervals within our study area [66]. This fire frequency is likely too high to detect individual fire events within our sediment cores (see [49,67]), given that our 1 cm sampling interval results in a 9–33-year resolution using the measured sedimentation rates of 0.03–0.11 cm $yr^{-1}$, for the depths where charcoal was counted (Table 3). Additionally, remobilization, transport, and deposition of charcoal from the drainage basin to our study sites was likely not significant; where the organic nature of the sediments suggests in situ deposition and a lack of mineral sediment deposition, which would involve transport. Since there was little surface drainage entering our depression marsh study sites, and no channels, a significant charcoal influx to the wetlands via surface water transport is unlikely (see Reference [42]) and the macroscopic charcoal present within the sites likely reflects local fires that occurred within close proximity (~1 km) of the sites (see Reference [22]).

The charcoal record from sites 1, 5, and 8 supported a pre-European high fire frequency interval that was within the 9–33-year sampling resolution, as charcoal is nearly ubiquitous at all sample depth intervals (Figures 5 and 6). Statistical analysis using the CharAnalysis program revealed eight fire events for site 1 and seven events for site 5 (Figure 6). However, there was abundant charcoal at nearly all sampling intervals and even the peaks extended for long periods of time, rather than being short and discrete as was found in other studies with fires that were less frequently spaced (e.g., References [44,68]). It seems logical that the fire events identified in the statistical analysis represent additional charcoal influx beyond the typical fire activity at the sites, perhaps related to climate variability, human activity, or other unknown causes. However, the fire record is not being decomposed into individual fires because fires are too frequent to distinguish given the sampling resolution. Closely spaced samples can represent one or more fires occurring years apart in areas of frequent burning and increasing the sample resolution (<1 cm) does not always improve the temporal resolution in temperate settings, likely because modest bioturbation masks the individual fire events [69]. Allen et al. [49] suggested that sedimentary charcoal records may actually underestimate fire frequency in mixed conifer settings with a high-frequency fire regime.

Charcoal is less concentrated in the upper part of the peat profile for sites 1 and 5, although two fire events were identified in the statistical analysis towards the top of the core for site 5 (Figures 5 and 6). Charcoal is often less concentrated in the uppermost portion of peat profiles because unhumified plant materials occupy a greater fraction of the samples [42]. The remainder of the fire record from sites 1 and 5 did not show a clear relationship in CHAR distributions between the two sites. Both sites generally had lower CHAR values from ca. 500 to 700 cal BP, with no identified fire events during that time window, and both sites had higher CHAR values with identified fire events from 350 to 450 cal BP. Other studies of macroscopic charcoal records at multiple sites often show that sites within close proximity to one another have unique fire histories [65,70], even when responding to the same climate change [71], although charcoal records are often correlated among multiple cores within a single deposit [49]. Thus, it may be best to view the charcoal records from sites 1 and 5 as a composite record, with CHAR values indicating generally high fire activity for the region through nearly the entire time period represented, with a possible decrease in activity from ca. 500 to 700 cal BP. However, charcoal was still present at all sampling intervals for both sites during this time of lower charcoal influx, so it is likely that fire was still prevalent. The CHAR record for site 8 also suggested high-frequency fires throughout the time period analyzed, even though age control was poor (Figure 5c).

While charcoal studies of sediments within a longleaf pine forest upland matrix are lacking, a study was conducted south of our field area, within the pine rockland ecosystem of the Florida Keys. Albritton's [72] microscopic and macroscopic charcoal analysis from the Big Pine Key, FL showed

frequent fire in the pine rockland ecosystem, supporting a hypothesis of 3–7-year return intervals and an increase in fire occurrence at 1200 cal BP. Our site 1 also showed increased fire activity near 1200 cal BP (Figures 5 and 6). Microscopic and macroscopic charcoal abundances indicated high fire activity in the Bahamas pine rocklands coeval with Big Pine Key [73], and a dendrochronological record from the Florida Keys suggested a 6–9-year burn interval [74]. Kocis [67] provides a ~4500 yr record of macroscopic charcoal for the pine rockland ecosystem of the Florida Keys and found evidence of a rapid fire return interval (within the approximately decadal sampling resolution), with all 1 cm sediment sampling increments containing macroscopic charcoal, similar to our study.

### *4.5. Carbon Storage*

We reported the first carbon sequestration rates determined for Florida depression marshes (Table 3). It is estimated that 20 to 30 percent of the global carbon storage in soils occurs within wetland systems [75]. We found carbon storage rates between 16 to 56 g $cm^{-2}$ $yr^{-1}$, depending on depth in the soil profile, with generally decreasing storage with depth (Table 3), which could be the result of long-term decomposition. These carbon sequestration rates are similar to an average rate determined for northern peatlands and are less than the typical rates determined for tropical and subtropical wetlands [75]. Based on an average carbon sequestration rate of 31 g $cm^{-2}$ $yr^{-1}$ and a total wetland area of the three depression marshes (~0.95 ha), we calculated a total annual accumulation of 293 kg of carbon in the three wetlands studied.

## 5. Conclusions

Hydroregime models for our study sites suggested shallower depths and shortened hydroperiods in the future, under one of many potential climate change scenarios [7]. Our study demonstrated that some depression marshes have maintained steady peat accumulation over the past several thousand years, probably due to relatively stable climate conditions and continually saturated soil, despite occasional brief periods when they were not inundated. Our bulk elemental and carbon isotopic results supported the idea of consistently wet soils at two of the three study sites over the past several thousand years. This peat accumulation certainly has its limits and the drier conditions at site 8 have likely led to peat loss. Data from site 8 suggested that peat oxidation was likely, when the water table more often falls below the soil surface, which may become the norm for depression marshes generally if climate conditions lead to drier sites. Increased soil drying episodes could also result in the loss of much of the carbon stock stored in wetland peat. Our sampling interval allowed for an approximately 10–30 year resolution, where evidence of fire was present in nearly all the samples from the three study sites. Our results indicated that fires were historically frequent within the longleaf pine-wiregrass sandhills ecosystem and supported the current prescribed burn management strategies based on the historical fire regimes.

**Author Contributions:** B.T. and C.H.G. conceptualized the study and were also involved with the study methodology, formal analysis, investigation, writing—original draft preparation, project administration, and funding acquisition. M.D. and J.C. conducted formal analysis, investigation, and writing—review and editing. D.S. was involved with funding acquisition and writing—review and editing.

**Funding:** This project was supported by a Faculty Summer Research Grant from Stetson University and a Provost's Funding Support Grant from Western Carolina University.

**Acknowledgments:** The field and lab support of Anais Seychelles, Blake Hartshorn, Carolina Lilly, and Jessica Floyd is gratefully acknowledged, as is the support of the many field technicians who collected weather and water depth data over the course of the 24 year monitoring study. Ocala National Forest Seminole Ranger District graciously provided access to the field sites. The thoughtful comments of three anonymous reviewers improved the manuscript and gratitude is hereby expressed for their service.

**Conflicts of Interest:** The authors declare no conflict of interest.

## References


1. Myers, R.L. Scrub and high pine. In *Ecosystems of Florida*; Myers, R.L., Ewel, J.J., Eds.; University of Central Florida Press: Orlando, FL, USA, 1990; pp. 150–193. ISBN 0813010225.
2. Watts, W.A.; Hansen, B.C.S. Pre-Holocene and Holocene pollen records of vegetation history from the Florida peninsula and their climatic implications. *Palaeogeogr. Palaeoclimatol. Palaeoecol.* **1994**, *109*, 163–176. [CrossRef]
3. Greenberg, C.H.; Collins, B.S.; McNab, W.H.; Miller, D.K.; Wein, G.R. Introduction to natural disturbances and historic range of variation: Type, frequency, severity, and post-disturbance structure in central hardwood forests. In *Natural Disturbances and Historic Range of Variation: Type, Frequency, Severity, and Post-Disturbance Structure in Central Hardwood Forests, USA*; Greenberg, C.H., Collins, B., Eds.; Managing Forest Ecosystem Series; Springer: Berlin, Germany, 2015; Volume 32, pp. 1–32. ISBN 978-3-319-21526-6.
4. FNAI—Florida Natural Areas Inventory. *Guide to the Natural Communities of Florida: 2010 Edition*; Florida Natural Areas Inventory: Tallahassee, FL, USA, 2010; 276p.
5. Wear, D.N.; Huggett, R.; Greis, J.G. Constructing alternative futures. In *The Southern Forest Futures Project: Technical Report*; Gfeneral Technical Report SRS-178; Wear, D.N., Greis, J.G., Eds.; USDA-Forest Service, Southern Research Station: Asheville, NC, USA, 2013; pp. 11–26.
6. Greenberg, C.H.; Zarnoch, S.J.; Austin, J.D. Weather, hydroregime, and breeding effort influence juvenile recruitment of anurans: Implications for climate change. *Ecosphere* **2017**, *8*, e01789. [CrossRef]
7. Greenberg, C.H.; Goodrick, S.; Austin, J.D.; Parresol, B.R. Hydroregime prediction models for ephemeral groundwater-driven sinkhole wetlands: A planning tool for climate change and amphibian conservation. *Wetlands* **2015**, *35*, 899–911. [CrossRef]
8. Quillen, A.K.; Gaiser, E.E.; Grim, E.C. Diatom-based paleolimnological reconstruction of regional climate and local land-use change from a protected sinkhole lake in southern Florida, USA. *J. Paleolimnol.* **2013**, *49*, 15–30. [CrossRef]
9. Alvarez Zarikian, C.A.; Swart, P.K.; Gifford, J.A.; Blackwelder, P.L. Holocene paleohydrology of Little Salt Spring, Florida, based on ostracod assemblages and stable isotopes. *Palaeogeogr. Palaeoclimatol. Palaeoecol.* **2005**, *225*, 134–156. [CrossRef]
10. Balsillie, J.H.; Donoghue, J.F. *High Resolution Sea Level History for the Gulf of Mexico since the Last Glacial Maximum*; Florida Geological Survey Report of Investigations No. 103; Florida Geological Survey: Tallahassee, FL, USA, 2004.
11. Simms, A.R.; Lambeck, K.; Purcell, A.; Anderson, J.B.; Rodriquez, A.B. Sea-level history of the Gulf of Mexico since the Last Glacial Maximum with implications for the melting history of the Laurentide Ice Sheet. *Quat. Sci. Rev.* **2007**, *26*, 920–940. [CrossRef]
12. Donoghue, J.F. Sea level history of the northern Gulf of Mexico coast and sea level rise scenarios for the near future. *Clim. Chang.* **2011**, *107*, 17–33. [CrossRef]
13. LaMoreaux, H.K.; Brook, G.A.; Knox, J.A. Late Pleistocene and Holocene environments of the southeastern United States from the stratigraphy and pollen content of a peat deposit on the Georgia coastal plain. *Palaeogeogr. Palaeoclimatol. Palaeoecol.* **2009**, *280*, 300–312. [CrossRef]
14. Gaiser, E.E.; Taylor, B.E.; Brooks, M.J. Establishment of wetlands on the southeastern Atlantic Coastal Plain: Paleolimnological evidence of a mid-Holocene hydrologic threshold from a South Carolina pond. *J. Paleolimnol.* **2001**, *26*, 373–391. [CrossRef]
15. Marlon, J.R.; Bartlein, P.J.; Daniau, A.-L.; Harrison, S.P.; Maezumi, S.Y.; Power, M.J.; Tinner, W.; Vanniére, B. Global biomass burning: A synthesis and review of Holocene paleofire records and their controls. *Quat. Sci. Rev.* **2013**, *65*, 5–25. [CrossRef]
16. Power, M.J. Changes in fire regimes since the Last Glacial Maximum: An assessment based on a global synthesis and analysis of charcoal data. *Clim. Dyn.* **2008**, *30*, 887–907. [CrossRef]
17. Power, M.J.; Bush, M.B.; Behling, H.; Horn, S.P.; Mayle, F.E.; Urrego, D.H. Paleofire activity in tropical America during the last 21 ka: A regional synthesis based on sedimentary charcoal. *PAGES News* **2010**, *18*, 73–75. [CrossRef]
18. Power, M.J.; Mayle, F.E.; Bartlein, P.J.; Marlon, J.R.; Anderson, R.S.; Behling, H.; Brown, K.J.; Carcaillet, C.; Colombaroli, D.; Gavin, D.G.; et al. Climatic control of the biomass-burning decline in the Americas after AD 1500. *Holocene* **2012**, *23*, 3–13. [CrossRef]

19. De LaFontaine, G.; Asselin, H. Soil charcoal stability over the Holocene across boreal northeastern North America. *Quat. Res.* **2011**, *76*, 196–200. [CrossRef]
20. De LaFontaine, G. Soil charcoal stability over the Holocene—Response to comments by Mikael Ohlson. *Quat. Res.* **2012**, *78*, 155–156. [CrossRef]
21. Peters, M.E.; Higuera, P.E. Quantifying the source area of macroscopic charcoal with a particle dispersal model. *Quat. Res.* **2007**, *67*, 304–310. [CrossRef]
22. Clark, J.S. Fire and climate change during the last 750 years in northwestern Minnesota. *Ecol. Monogr.* **1990**, *60*, 135–159. [CrossRef]
23. Carcaillet, C.; Bouvier, M.; Fréchette, B.; Larouche, A.; Richard, P.J.H. Comparison of pollen-slide and sieving methods in lacustrine charcoal analyses for local and regional fire history. *Holocene* **2001**, *11*, 467–476. [CrossRef]
24. Ohlson, M.; Tryterud, E. Interpretation of the charcoal record in forest soils: Forest fires and their production and deposition of macroscopic charcoal. *Holocene* **2000**, *10*, 519–525. [CrossRef]
25. Gavin, D.G.; Hu, F.S.; Lertzman, K.; Gorbett, P. Weak climatic control of stand-scale fire history during the Late Holocene. *Ecology* **2006**, *87*, 1722–1732. [CrossRef]
26. Long, C.J.; Whitlock, C.; Bartlein, P.J.; Millspaugh, S.H. A 9000-year fire history from the Oregon Coast Range, based on a high-resolution charcoal study. *Can. J. For. Res.* **1998**, *28*, 774–787. [CrossRef]
27. Conedera, M.; Tinner, W.; Neff, C.; Meurer, M.; Dickens, A.F.; Krebs, P. Reconstructing past fire regimes: Methods, applications, and relevance to fire management and conservation. *Quat. Sci. Rev.* **2009**, *28*, 435–456. [CrossRef]
28. Higuera, P.E.; Brubaker, L.B.; Anderson, P.M.; Hu, F.S.; Brown, T.A. Vegetation mediated the impacts of postglacial climate change on fire regimes in the south-central Brooks Range, Alaska. *Ecol. Monogr.* **2009**, *79*, 201–219. [CrossRef]
29. Zhang, H.; Zhang, Y.; Kong, Z.; Yang, Z.; Li, Y.; Tarasov, P.E. Late Holocene climate change and anthropogenic activities in north Xinjiang: Evidence from a peatland archive, the Caotanhu wetland. *Holocene* **2015**, *25*, 323–332. [CrossRef]
30. Gavin, D.G.; Hallet, D.J.; Hu, F.S.; Lertzman, K.P.; Pritchard, S.J.; Brown, K.J.; Lynch, J.A.; Bartlein, P.; Peterson, D.L. Forest fire and climate change in wetern North America: Insights from sediment charcoal records. *Front. Ecol. Environ.* **2007**, *5*, 499–506. [CrossRef]
31. Tanner, B.R.; Lane, C.S.; Martin, E.M.; Young, R.; Collins, B. Sedimentary proxy evidence of a mid-Holocene hypsithermal event in the location of a current warming hole, North Carolina, USA. *Quat. Res.* **2015**, *83*, 315–323. [CrossRef]
32. Meyers, P.A. Preservation of elemental and isotopic source identification of sedimentary organic matter. *Chem. Geol.* **1994**, *114*, 289–302. [CrossRef]
33. Fletcher, M.-S.; Cadd, H.R.; Haberle, S.G. Can we infer vegetation change from peat carbon and nitrogen content? A palaeoecological test from Tasmania, Australia. *Holocene* **2015**, *25*, 1802–1810. [CrossRef]
34. Ehleringer, J.R.; Cerling, T.E.; Helliker, B.R. C4 photosynthesis, atmospheric $CO_2$, and climate. *Oecologia* **1997**, *112*, 285–299. [CrossRef] [PubMed]
35. Farquhar, G.D.; Ehleringer, J.R.; Hubick, K.T. Carbon isotope discrimination and photosynthesis. *Annu. Rev. Plant Physiol. Plant Mol. Biol.* **1989**, *40*, 503–537. [CrossRef]
36. Teeri, J.A.; Stowe, L.G. Climatic patterns and the distribution of C4 grasses in North America. *Oecologia* **1976**, *23*, 1–12. [CrossRef] [PubMed]
37. Teeri, J.A.; Stowe, L.G.; Livingstone, D.A. The distribution of C4 species of the cyperaceae in North America in relation to climate. *Oecologia* **1980**, *47*, 307–310. [CrossRef] [PubMed]
38. NOAA. Available online: http://www.ncdc.noaa.gov/data-access/land-based-station-data/land-based-datasets/climate-normals (accessed on 5 December 2017).
39. Scott, T.M. The Cypresshead Formation in northern peninsular Florida. In *Southeastern Geological Society Annual Field Trip Guidebook*; Pirkle, F.L., Reynolds, J.G., Eds.; Southeastern Geological Society: Tallahassee, FL, USA, 1988; pp. 70–72.
40. Soil Survey Staff, Official Soil Series Descriptions, Natural Resources Conservation Service. United States Department of Agriculture. Available online: https://www.nrcs.usda.gov/wps/portal/nrcs/detail/soils/home/?cid=nrcs142p2_053587 (accessed on 5 December 2017).

41. Reimer, P.J. IntCal13 and Marine13 radiocarbon age calibration curves, 0–50,000 years cal BP. *Radiocarbon* **2013**, *55*, 1869–1887. [CrossRef]
42. Mooney, S.D.; Tinner, W. The analysis of charcoal in peat and organic sediments. *Mires Peat* **2011**, *7*, 1–18.
43. Schlachter, K.J.; Horn, S.P. Sample preparation methods and replicability in macroscopic charcoal analysis. *J. Paleolimnol.* **2010**, *44*, 701–708. [CrossRef]
44. Ali, A.A.; Higuera, P.E.; Bergeron, Y.; Carcaillet, C. Comparing fire-history interpretations based on area, number and estimated volume of macroscopic charcoal in lake sediments. *Quat. Res.* **2009**, *72*, 462–468. [CrossRef]
45. Whitlock, C.; Millspaugh, S.H. Testing the assumptions of fire-history studies: An examination of modern charcoal accumulation in Yellowstone National Park, USA. *Holocene* **1996**, *6*, 7–15. [CrossRef]
46. Schlacher, T.A.; Connolly, R.M. Effects of acid treatment on carbon and nitrogen stable isotope ratios in ecological samples: A review and synthesis. *Methods Ecol. Evol.* **2014**, *5*, 541–550. [CrossRef]
47. Higuera, P.E.; Brubaker, L.B.; Anderson, P.M.; Brown, T.A.; Kennedy, A.T.; Hu, F.S. Frequent fires in ancient shrub tundra: Implications of paleorecords for arctic environmental change. *PLoS ONE* **2008**, *3*, e0001744. [CrossRef] [PubMed]
48. Frost, C.C. Presettlement fire regimes in southeastern marshes, peatlands, and swamps. In *Fire in Wetlands: A Management Perspective, Proceedings of the 19th Tall Timbers Fire Ecology Conference*; Cerulean, S.I., Engstrom, T., Eds.; Tall Timbers Research Inc.: Tallahassee, FL, USA, 1995; Volume 19, pp. 39–60.
49. Allen, C.D.; Anderson, R.S.; Jass, R.B.; Toney, J.L.; Baisan, C.H. Paired charcoal and tree-ring records of high-frequency Holocene fire from two New Mexico bog sites. *Int. J. Wildl. Fire* **2008**, *17*, 115–130. [CrossRef]
50. Minckley, T.A.; Clementz, M.T.; Brunelle, A.; Klopfenstein, G.A. Isotopic analysis of wetland development in the American Southwest. *Holocene* **2009**, *19*, 737–745. [CrossRef]
51. Meyers, P.A. Organic geochemical proxies of paleoceanographic, paleolimnologic, and paleoclimatic processes. *Org. Geochem.* **1997**, *5*, 213–250. [CrossRef]
52. Willard, D.A.; Bernhardt, C.E. Impacts of past climate and sea level change on Everglades wetlands: Placing a century of anthropogenic change into a late-Holocene context. *Clim. Chang.* **2011**, *107*, 59–80. [CrossRef]
53. Harley, G.L.; Maxwell, J.T.; Larson, E.; Grissino-Mayer, H.D.; Henderson, J.; Huffman, J. Suwannee River flow variability 1550-2005 CE reconstructed from a multispecies tree-ring network. *J. Hydrol.* **2017**, *544*, 438–451. [CrossRef]
54. Emiliani, C.; Gartner, S.; Lidz, B.; Eldridge, K.; Elvey, D.K.; Huang, T.C.; Stipp, J.J.; Swanson, M.F. Paleoclimatological analysis of Late Quaternary cores from the northeastern Gulf of Mexico. *Science* **1975**, *189*, 1083–1088. [CrossRef] [PubMed]
55. Poore, R.Z.; Dowsett, H.J.; Verado, S.; Quinn, T.M. Millennial- to century-scale variability in Gulf of Mexico Holocene climate records. *Paleoceanography* **2003**, *18*, 1048. [CrossRef]
56. Grimm, E.C.; Jacobson, G.L., Jr.; Watts, W.A.; Hansen, B.C.S.; Maasch, K.A. A 50,000-year record of climate oscillations from Florida and its temporal correlation with the Heinrich events. *Science* **1993**, *261*, 198–200. [CrossRef] [PubMed]
57. Watts, W.A. A pollen diagram from Mud Lake, Marion County, north-central Florida. *GSA Bull.* **1969**, *80*, 631–642. [CrossRef]
58. Watts, W.A. Postglacial and interglacial vegetation history of southern Georgia and central Florida. *Ecology* **1971**, *52*, 676–690. [CrossRef] [PubMed]
59. Watts, W.A.; Stuiver, M. Late Wisconsin climate of northern Florida and the origin of species-rich deciduous forest. *Science* **1980**, *210*, 325–327. [CrossRef] [PubMed]
60. Watts, W.A.; Hansen, B.C.S.; Grimm, E.C. Camel Lake: A 40 000-YR record of vegetational and forest history from northwest Florida. *Ecology* **1992**, *73*, 1056–1066. [CrossRef]
61. Delcourt, H.R.; Delcourt, P.A. Pre-Columbian Native American use of fire on Southern Appalachian landscapes. *Conserv. Biol.* **1997**, *11*, 1010–1014. [CrossRef]
62. Frost, C.C. Presettlement fire frequency regimes of the United States: A first approximation. In *Fire in Ecosystem Management: Shifting the Paradigm from Suppression to Prescription, Proceedings of the Tall Timbers Fire Ecology Conference*; Pruden, T.L., Brennan, L.A., Eds.; Tall Timbers Research Inc.: Tallahassee, FL, USA, 1998; Volume 20, pp. 70–81.
63. Stambaugh, M.C.; Guyette, R.P.; Marschall, J.M. Longleaf pine (*Pinus palustris* Mill.) fire scars reveal new details of a frequent fire regime. *J. Veg. Sci.* **2011**, *22*, 1094–1104. [CrossRef]

64. White, C.R.; Harley, G.L. Historical fire in longleaf pine (*Pinus palustris*) forests of south Mississippi and its relation to land use and climate. *Ecosphere* **2016**, *7*, e01458. [CrossRef]
65. Kasin, I.; Blanck, Y.; Storaunet, K.O.; Rolstad, J.; Ohlson, M. The charcoal record in peat and mineral soil across a boreal landscape and possible linkages to climate change and recent fire history. *Holocene* **2013**, *23*, 1052–1065. [CrossRef]
66. Fs.usda.gov, Ocala National Forest Begins 2016 Prescribed Fire Season. Available online: https://www.fs.usda.gov/detail/ocala/news-events/?cid=FSEPRD484958 (accessed on 7 December 2017).
67. Kocis, D.L. Reconstruction of Fire History in the National Key Deer Refuge, Monroe County, Florida, USA: The Palmetto Pond Macroscopic Charcoal Record. Master's Thesis, University of Tennessee, Knoxville, TN, USA, 2012, 99p.
68. Crausbay, S.D.; Higuera, P.E.; Sprugel, D.G.; Brubaker, L.B. Fire catalyzed rapid ecological change in lowland coniferous forests of the Pacific Northwest over the past 14,000 years. *Ecology* **2017**, *98*, 2356–2369. [CrossRef] [PubMed]
69. Whitlock, C.; Larsen, C. Charcoal as a fire proxy. In *Tracking Environmental Change Using Lake Sediments. Volume 3: Terrestrial, Algal, and Siliceous Indicators*; Smol, J.P., Birks, H.J.B., Last, W.M., Eds.; Kluwer Academic Publishers: Dordrecht, The Netherlands, 2001; pp. 75–97. ISBN 978-1-4020-0681-4.
70. Ohlson, M.; Korbøl, A.; Økland, R.H. The macroscopic charcoal record in forested boreal peatlands in southeast Norway. *Holocene* **2006**, *16*, 731–741. [CrossRef]
71. Sugimura, W.Y.; Sprugel, D.G.; Brubaker, L.B.; Higuera, P.E. Millennial-scale changes in local vegetation and fire regimes on Mount Constitution, Orgas Island, Washington, USA, using small hollow sediments. *Can. J. For. Res.* **2008**, *38*, 539–552. [CrossRef]
72. Albritton, J.W. A 1700-Year History of Fire and Vegetation in Pine Rocklands of National Key Deer Refuge, Big Pine Key, Florida: Charcoal and Pollen Evidence from Key Deer Pond. Master's Thesis, University of Tennessee, Knoxville, TN, USA, 2009, 110p.
73. West, D. Late Holocene Charcoal Stratigraphy and Modern Charcoal Deposition in the Pine Rocklands of Great Abaco Island, the Bahamas. Master's Thesis, University of Tennessee, Knoxville, TN, USA, 2007, 78p.
74. Harley, G.L.; Grissino-Mayer, H.D.; Horn, S.P. Fire history and forest structure of an endangered subtropical ecosystem in the Florida Keys, USA. *Int. J. Wildl. Fire* **2013**, *22*, 394–404. [CrossRef]
75. Mitsch, W.J.; Gosselink, J.G. *Wetlands*, 5th ed.; John Wiley & Sons: Hoboken, NJ, USA, 2015; 456p, ISBN 978-1-118-67682-0.